



**POLITECNICO**  
MILANO 1863

SCUOLA DI INGEGNERIA INDUSTRIALE  
E DELL'INFORMAZIONE

EXECUTIVE SUMMARY OF THE THESIS

## State of the art and analysis of open-end winding motor drives

LAUREA MAGISTRALE IN ELECTRICAL ENGINEERING - INGEGNERIA ELETTRICA

**Author:** MICHELE FASLIROLI

**Advisor:** PROF. MARIA STEFANIA CARMELI

**Academic year:** 2022-2023

### 1. Introduction

In recent years, especially in order to cope with climate change problems, electrification in traction applications through the introduction of electric motors in various types of vehicles, such as trains and cars, is becoming increasingly evident. Thanks to this trend, there is a continuous research into more advanced and efficient technologies, including the motors used in BEVs and HEVs (battery electric vehicles and hybrids electric vehicles, respectively). Thanks to their high efficiency and excellent low-speed torque, the permanent magnets synchronous motors (PMSM) are being more widely used in EVs.

In the study performed, a new configuration of this type of electrical machine was analysed, that of open-winding motors (OW). This kind of motor is obtained from conventional versions by opening the neutral point of the stator winding, usually connected in a star or delta configuration. In this way, two different three-phase inputs can be connected to an equal number of independent inverters, resulting in a dual-inverter configuration.

### 2. Open-end winding motor

The open-end winding typology is obtained from conventional AC brushless motors by opening

the neutral point on the stator winding, resulting in six different ends. These are fed by two independent inverters, that can be connected to two separate or a common voltage source, as in the configurations shown in Figure 1.

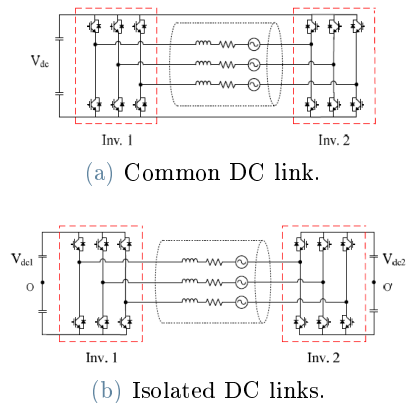


Figure 1: Analysed dual-inverter configurations [1].

An energy conversion device and an energy storage system, i.e. a battery and a floating capacitor, can also be connected on the DC-link. Configuration with two independent DC sources avoids the zero-sequence current that causes high Joule losses and ripple currents in the system. On the other hand, a single source reduces the cost, complexity and overall size of the setup [1].

The main benefit of the open-end winding motor is that it eliminates the need for a DC/DC converter, greatly reducing system complexity, cost and total power consumption.

It is necessary to introduce power management between the two sides of the motor, which optimises the power flow and the use of voltage sources, but with a higher complexity for the control system.

On the other hand, one of the main drawbacks of this configuration is that it greatly increases losses due to the switching frequency. There is also an increase in system costs due to the higher number of components involved and a rise in total volume.

The configuration that will be proposed in this study is the one shown in Figure 2, therefore with two isolated DC voltage sources connected to the dual-inverter.

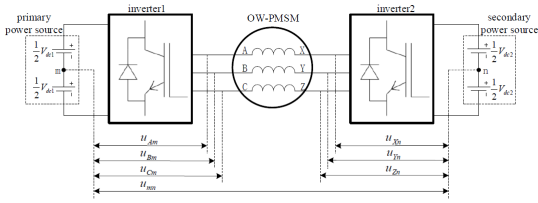


Figure 2: System diagram with dual-inverter and two independent DC sources.

The applied voltage at the ends of the open-end winding motor will be given by the difference between the voltage vectors  $u_{s1}$  and  $u_{s2}$  generated by the two inverters, as described in the equation (1).

$$\vec{u}_s = \vec{u}_{s1} - \vec{u}_{s2}, \quad (1)$$

$$\vec{u}_s = \sqrt{\frac{2}{3}}(u_{AX}e^{j0} + u_{BY}e^{j\frac{2\pi}{3}} + u_{CZ}e^{j\frac{4\pi}{3}}).$$

The model of this type of motor coincides with that used for conventional permanent magnet synchronous machines, described by the system of mathematical equations (2):

$$\left\{ \begin{array}{l} v_{sd} = R_s i_{sd} + L_d p i_{sd} - \dot{\theta}_m L_q i_{sq}, \\ v_{sq} = R_s i_{sq} + L_q p i_{sq} - \dot{\theta}_m L_d i_{sd} + \dot{\theta}_m \psi_{pm}, \\ \psi_{sd} = L_d i_{sd} + \psi_{pm}, \\ \psi_{sq} = L_q i_{sq}, \\ \frac{d}{dt} \dot{\theta}_m = \frac{n_p}{J} (T_e - T_r), \\ T_e = n_p [(L_d - L_q) i_{sd} i_{sq} + \psi_{pm} i_{sq}]. \end{array} \right. \quad (2)$$

In which,  $v_{sd}$ ,  $v_{sq}$ ,  $i_{sd}$ ,  $i_{sq}$ ,  $\psi_{sd}$ ,  $\psi_{sq}$  are respectively the stator voltage, current and flux components in the  $dq$ -axis,  $R_s$  is the stator re-

sistance,  $\psi_{pm}$  is the flux generated by the permanent magnets and  $n_p$  the pole pairs,  $J$  is the equivalent inertia,  $T_r$  and  $T_e$  are the load's resistant and the electromagnetic torque and  $\dot{\theta}_m$  is the derivative of the mechanical angle, between the d-axis and the magnetic axis of the motor. The case of an isotropic machine ( $L_d = L_q = L_s$ ) will also be considered.

### 3. System configuration

In order to test whether open-end winding motors can actually be a solution for improving the efficiency and growth of electric vehicles, a control system must be introduced to exploit the benefits and to minimise the disadvantages.

In order to do this, the control proposed in [2] was implemented, in which a space vector modulation based on a look-up table is used for the dual-inverter configuration. This method is designed to minimise the switching losses. Moreover, this control method is able to maximise the output power of the motor and, at the same time, reduce current harmonics, so as to further minimise losses in the system.

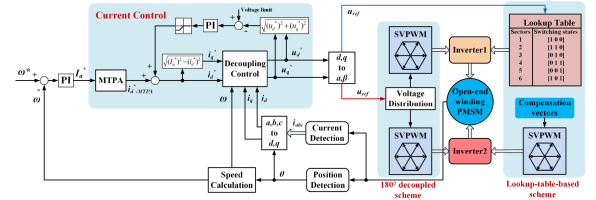


Figure 3: Overall control scheme diagram of the implemented solution [2].

As shown in Figure 3, the switching states of the first voltage source inverter (VSI) are handled with a six-step method according to the lookup table 1. Based on the position of the reference voltage, it identifies in which of the six sectors of the plane  $\alpha\beta$  the vector  $\bar{u}_{ref}$  is located.

Sector	Ref. Voltage's Angle	Switching States
I	$-30^\circ \leq \theta < 30^\circ$	[1 0 0]
II	$30^\circ \leq \theta < 90^\circ$	[1 1 0]
III	$90^\circ \leq \theta < 150^\circ$	[0 1 0]
IV	$150^\circ \leq \theta < 180^\circ$	[0 1 1]
V	$-150^\circ \leq \theta < -90^\circ$	[0 0 1]
VI	$-90^\circ \leq \theta < -30^\circ$	[1 0 1]

Table 1: Inverter1 switch status according to the reference voltage angle.

On the other hand, the second VSI will work as a compensation inverter with the task of balancing the power flow in the system. Always depending on the angle  $\theta_{u_{ref}}$ , the new components in the stationary reference plane  $\alpha\beta$  for inverter2 are generated, according to the relations shown in Table 2.

Sector	Compensation Vectors
I	$u_{\alpha 2}^* = u_{\alpha}^* - \frac{2}{3}V_{dc1}$ ; $u_{\beta 2}^* = u_{\beta}^*$
II	$u_{\alpha 2}^* = u_{\alpha}^* - \frac{1}{3}V_{dc1}$ ; $u_{\beta 2}^* = u_{\beta}^* - \frac{\sqrt{3}}{3}V_{dc1}$
III	$u_{\alpha 2}^* = u_{\alpha}^* + \frac{1}{3}V_{dc1}$ ; $u_{\beta 2}^* = u_{\beta}^* - \frac{\sqrt{3}}{3}V_{dc1}$
IV	$u_{\alpha 2}^* = u_{\alpha}^* + \frac{2}{3}V_{dc1}$ ; $u_{\beta 2}^* = u_{\beta}^*$
V	$u_{\alpha 2}^* = u_{\alpha}^* + \frac{1}{3}V_{dc1}$ ; $u_{\beta 2}^* = u_{\beta}^* + \frac{\sqrt{3}}{3}V_{dc1}$
VI	$u_{\alpha 2}^* = u_{\alpha}^* - \frac{1}{3}V_{dc1}$ ; $u_{\beta 2}^* = u_{\beta}^* + \frac{\sqrt{3}}{3}V_{dc1}$

Table 2: Components of the compensation voltage vector of inverter2.

The compensation voltage vector obtained will be used in the SVPWM to get the switching states of the second inverter, and thus the voltage it will generate. The control strategy analysed for the open-end winding motor will be compared with a conventional  $180^\circ$  decoupled modulation. It generates two vectors with a magnitude equal to half the reference voltage, but with an opposite angle, as shown in Figure 4. They are then fed into two SVPWM calculation modules to generate the switching states of the dual-inverter.

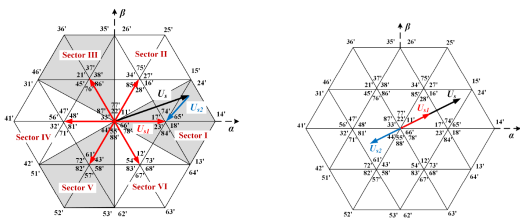


Figure 4: Space vector modulation diagram of the lookup table method and  $180^\circ$  decoupled strategy.

## 4. System model implementation

To realise the control of the open-end winding motor, a block diagram was used consisting of two closed loops, one current loop and the other speed loop, as shown in Figure 5. It is based on the voltage equations of the system 2 to generate the components of the stator reference voltage

$u_s ref$ .

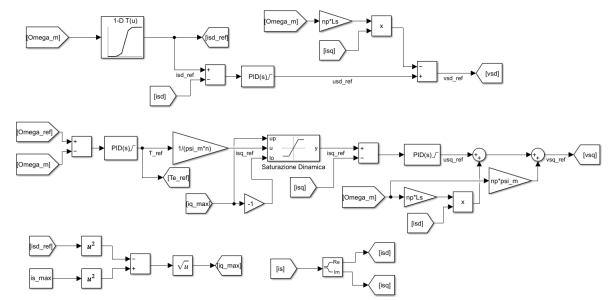


Figure 5: Block diagram for the dq-axis stator voltage components.

In order to obtain the currents  $i_{sd ref}$  and  $i_{sq ref}$ , and to comply with the operating regions of the motor, a flux-weakening control was used. For speeds lower than the base speed  $\omega_b$ , a constant torque zone occurs as the current  $i_{sd}$  is kept equal to zero, while  $i_{sq}$  will coincide with the maximum value of the stator current, imposed by the thermal limits of the motor. Instead, with  $\omega > \omega_b$ , the current  $i_{sd}$  will take negative values to counteract the increase emf  $E$  induced, while the  $i_{sq}$  will have to decrease to respect the thermal constraint limits of the motor current. Thus, there will also be a decrease in the electromagnetic torque.

These operating regions have been implemented in the model via a MatLab script, and they handle the value of  $i_{sd ref}$ . Instead, the  $i_{sq ref}$  current is derived from the  $T_e$  required to keep the mechanical speed equal to the reference one.

### 4.1. Lookup table-based modulation

After deriving the stator reference voltage, it is converted into the corresponding  $\alpha\beta$  reference frame components.

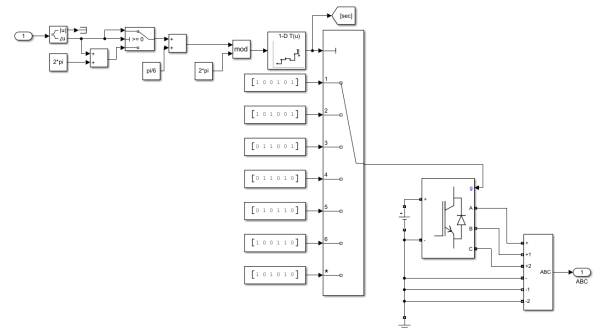


Figure 6: Control system used for Inverter1.

In this way, it is possible to derive through the

six-step method in which sector the stator vector  $\bar{v}_{\alpha\beta}$  is positioned, generating the switching states of inverter1, as visible in Figure 6. The look-up table 1 was introduced into the system to achieve this.

Instead, a space vector PWM is applied to handle the switching states of inverter2, as represented in Figure 7. It receives as input the compensation voltage vector generated according to the relationships described in Table 2.

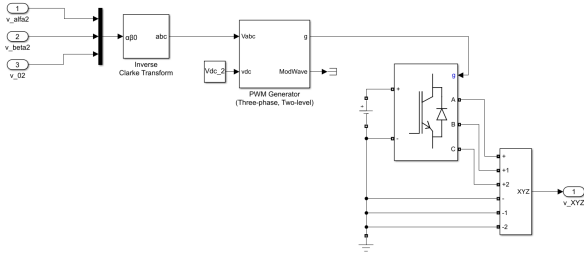


Figure 7: Control diagram applied to Inverter2.

The two three-phase voltages generated by the dual-inverter configuration are fed into the open-end winding motor model, which implements the equations (2) and (1).

#### 4.2. 180° decoupled SVPWM

To perform modulation using the conventional 180° decoupled scheme, the components of the reference vector  $\bar{v}_s$  are halved to obtain two three-phase voltages with the same amplitude but opposite angles. As can be seen in Figure8, they are used by the respective SVPWM to generate the switching states of the dual-inverter.

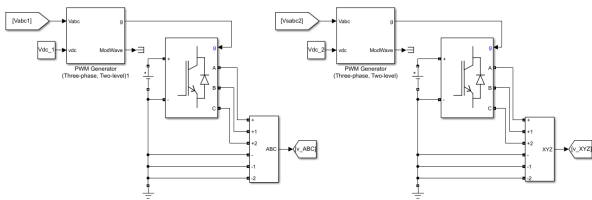


Figure 8: SVPWMs scheme for the dual-inverter.

### 5. Simulations

The lookup table-based modulation was compared with the 180° decoupled strategy via Simulink simulations, using the parameters in Table 3. These two types of control were analysed over the entire motor operating area, obtaining the trends shown in Figure 9. Therefore,

Parameter Name	Value
Stator resistance $R_s$	0.1 $\Omega$
Stator inductance $L_s$	0.8 mH
Permanent magnet flux $\psi_{pm}$	0.5 Wb
Pole pairs $n_p$	2
Rated power $P_m$	180 kW
DC-link voltage $V_{dc 1}$	200 V
DC-link voltage $V_{dc 2}$	200 V
Maximum electromagnetic torque $T_{e max}$	632 Nm
Base speed $\omega_b$	330.2 rad/s

Table 3: Motor and system parameters.

lookup table modulation has proved to be the most convenient solution, as it is able to reduce switching losses and total system complexity in comparison to the 180° decoupled scheme.

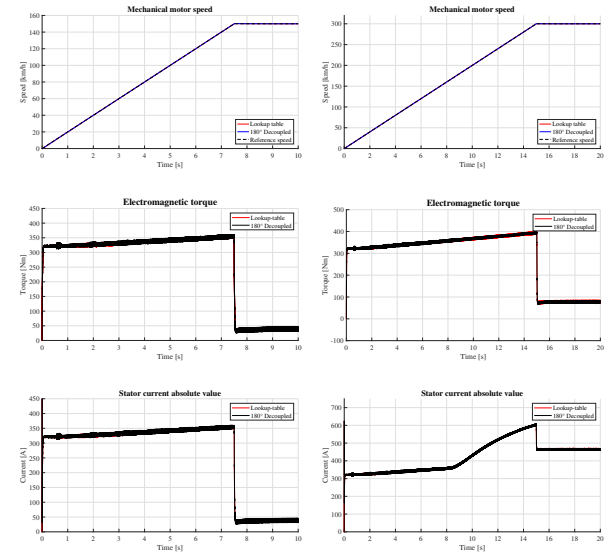


Figure 9: Motor quantities trends for the two strategies analysed, for  $\Omega < \Omega_b$  (right) and  $\Omega > \Omega_b$  (left)

Lastly, the proposed modulation of the OW motor was compared with that of a conventional PMSM on a traction application, using telemetry data from an EV during a lap at the Varano track.

As can be seen from the graphs in Figure 10, the trends associated with the open-end winding motor comply with the limits set in the operating regions and also follow the references appropriately, showing that the control part has also been implemented properly.

Again, the performance of the two motor types coincides. But, through hybrid six-step and pulse width modulation strategy it is possible to achieve the benefits of the dual-inverter configuration, such as the absence of a DC/DC con-

verter, better reliability and flexibility in the system.

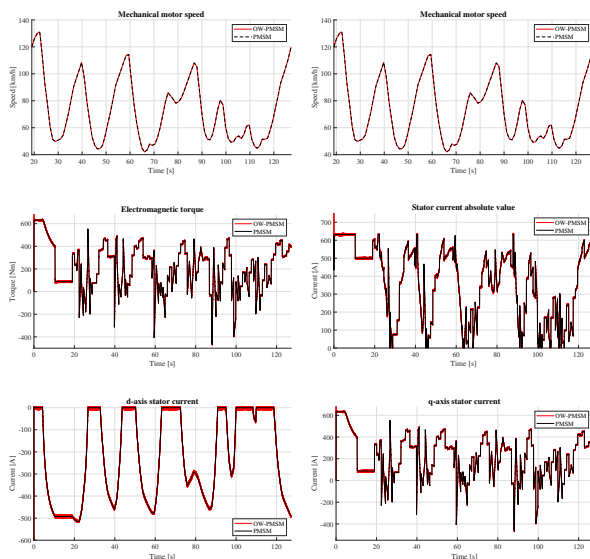


Figure 10: Comparison between OW-PMSM and a classic PMSM

## 6. Conclusions

In the study conducted, the open-end winding motors were analysed and a modulation technique, based on a look-up table, was proposed to underline the benefits that could be obtained by implementing this type of motor in EVs. It has proven to be better than the  $180^\circ$  decoupled strategy since, the use of hybrid modulation combining six-step and PWM allows a lower switching frequency of the first inverter and minimises overall losses in the system.

Furthermore, simulations have shown that by implementing this control on a dual-inverter configuration, with equal performance achieved, an improvement in efficiency and a reduction in complexity and cost, compared to a conventional control system, can be obtained.

## 7. Acknowledgements

First of all, I wanted to thank Professor Maria Stefania Carmeli and Professor Marco Mauri for giving me the opportunity to do my graduation thesis on a subject that I have always been passionate about and, for having given me a hand during the most difficult moments in the realisation of this study. In addition to them, I would also like to thank all the professors who

contributed to improving my knowledge during these five years at the Politecnico, especially those who made me passionate about the electrical machine field and their applications.

My biggest thanks go to my parents who have given me the opportunity to study at the Politecnico di Milano and, together with my brother, for encouraging and supporting me in every moments.

## References

- [1] Lee Yongjae and Ha Jung-Ik. Power enhancement of dual inverter for open-end permanent magnet synchronous motor. *IEEE Applied Power Electronics*, 2013.
- [2] Jing Wang and Jianhua Wu. Space vector modulation based on lookup table for a dual-inverter-fed open-end winding pmsm drive. *IEEE Vehicle Power and Propulsion Conference*, 2016.